



INTERNATIONAL JOURNAL OF SCIENCE FOR GLOBAL SUSTAINABILITY
**Experimental Design and Implementation of AC – DC Handset Travel
Charger**

*Yahaya Yusuf¹, Ismail Garba Sa'idu² and Buhari Maiyama Abdullahi³

¹Department of Physics, Zamfara College of Arts and Science Gusau, Nigeria

²Department of Physics, Usmanu Danfodio University Sokoto, Nigeria

³Department of Science Technology, Waziri Umaru Federal Polytechnic Birnin Kebbi, Nigeria

Corresponding Authors Email Address & Phone No.: bazata70@gmail.com; +2347034909425

Received on: October, 2020

Revised and Accepted on: November, 2020

Published on: December, 2020

ABSTRACT

Handset charger is device which charges a cellphone from an available direct current (DC) source. Moreover, a DC cellphone charger forms as an integral part of a cellphone package which is being used in conjunctions with an alternating current (AC) power supply. A simple off-line fly back switch mode buck converter charger is designed and implemented to charge cell phone from an AC source. The circuit is targeted to operate on universal input voltage range of 85 to 265 V AC. Minimizing cost and size, the circuit was designed to operate on a high frequency transformer. The design was first conducted on MULTISIM software to ascertain its working conditions before the construction procedure. Tools and materials were chosen based on their simplicity and availability in most of our local electronics shops. The charger was tested on different cell phones and found working satisfactory. The performance analysis shows that its power rating is about 4 watts.

Keywords: Direct current, Alternating current, Buck converter, High frequency transformer

1.0 INTRODUCTION

Most of the electronic devices are dependent on power charger. Battery chargers vary from different applications. It can be the mobile phone chargers, vehicles battery chargers, electric vehicle batteries chargers and also charging stations (Shobana, G. and Suguna, M. 2019). A current-limited power supply maintains a constant voltage across the battery (approximately 2.4V/cell, as specified by the battery manufacturer) until the charging current decreases below a current threshold defined by the capacity of the battery. At this point, the charger is placed in a trickle-charge mode (Christine, 2011).

Mobile phone plays an important role in communication. Almost all Portable electronic devices are battery powered; eventually they must be charged using the wired chargers (Joe, 2018 *et al*). There are several researches on the design and construction of cell phone chargers. Crosby & Deppong (2013) has designed and tested a wireless phone charger. Venkatesh and Chappidi (2015) designed a Portable USB Mobile Charger that uses power from the DC AA batteries instead of using the conventional power from the AC source. Francisco, *et al* (2019) also designed and constructed a multi-purpose hand crank mechanical energy charger. However mobile phones always

facing the difficulty of battery charging while travelling from one place to another (Kharudin *et al.*, 2016). Apart of being smaller and lighter in weight, switch mode power supply (SMPS) has a greater efficiency. Because the switching transistor dissipates little power in the saturated state and the off state compared to the active region. In this article a simple AC to DC travel handset charger circuit is been designed and experimentally implemented. It was built with few components that are available in most of electronics shops. Red light emitting diode (LED) indicator is ON to shows that the charger is connected to the mains, while green LED is ON to shows that charging is completed. It is designed to operate from low voltage of 85 to 220 volt.

2.0 THEORY

Linear supplies are still an option even in the current switch-mode dominant environment. If a design can accept the lower efficiency of a linear supply, its benefits may be appreciably. The major advantages of a linear supply are simplicity of design, lower cost, abundant relevant components, proven techniques, and low electromagnetic interference (EMI) emissions. While on the other hand, switch-mode designs are inherently noisy, and the circuits to be powered may be susceptible to that noise. The advantages of a switch-mode

power supply are just too great to ignore. Efficiency is the primary benefit of SMPS, which was found to be more than 90% for many designs. Small size and reasonable cost are other benefits (Lou, 2017).

From Ohms law Power (P) developed by an electrical circuit is giving by $P = IV = V^2/R$

2.1

Where; (I) is the current flowing in the circuit and (V) the potential difference across the two points.

Two basic types of switching regulators constitute the foundation of all of the pulse width-modulated (PWM) switching regulators. These types are the forward-mode regulators and the fly back-mode regulators. The name of each type is derived from

the way the magnetic elements are used within the regulator. Although they may resemble each other schematically, they operate in quite different fashions (Brown, 1990). Switched Mode Power Supply can be a complicated circuit, as can be seen from the block diagram shown in Figure 2.1. The AC supply is first rectified, and then filtered by the input reservoir capacitor to produce a rough DC input supply. This level can fluctuate widely due to variations in the mains. In addition the capacitance on the input has to be fairly large to hold up the supply in case of a severe drop in the mains. The SMPS can also be configured to operate from any suitable DC input; in this case the supply is called a DC to DC converter. (Humphreys *et al*, 1994)

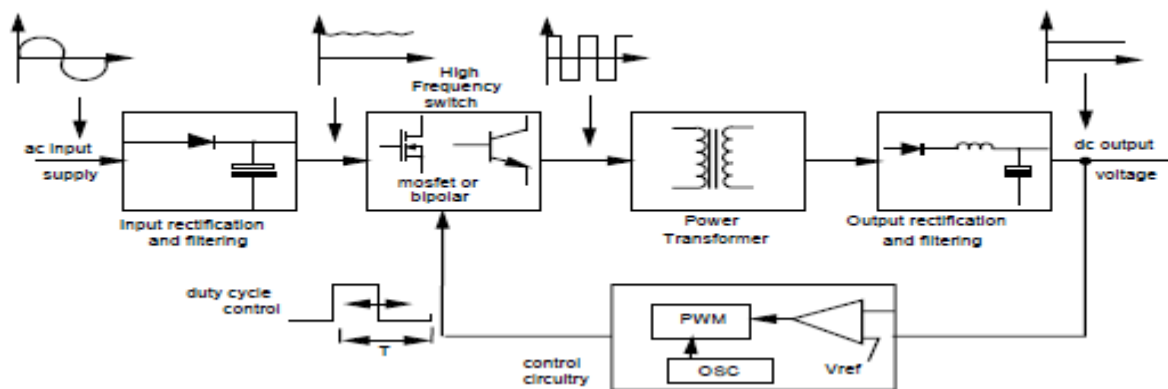


Figure: 2.1 Block diagram of basic switched mode power supply (Humphreys *et al*, 1994)

3.0 MATERIALS AND METHOD

3.1 Design Implementation

Figure 3.1 shows the block diagram of the cellphone charger. The AC Supply unit supplies power to the whole system. It is converted to DC directly by a half wave rectifier and smoothing by an electrolytic capacitor of higher potential

difference (PD). Switching action was performed by a transistor that switches across primary windings of the ferric core transformer. The PD on the bulk circuit is being control by the feedback circuitry.

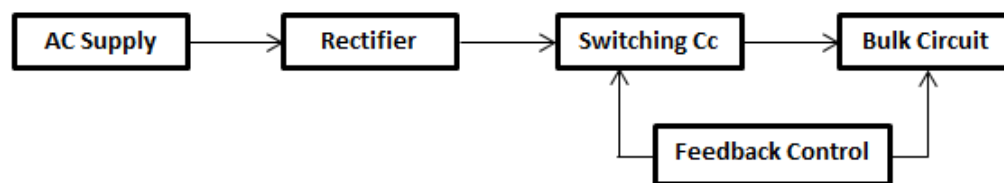


Figure: 3.1 Block diagram of the setup

3.2 Choice of the Switch Circuit

The switching action is performed by a high voltage and fast switching transistor. Since the power requirement is low, the MJE13001 transistor was chosen for this study. It has a collector base voltage (V_{CBO}) of 600 V, and collector current (I_C) of 200mA. It is mainly used in devices for powering and recharging various electronic gadgets (MJE13001 datasheet, 2015). However, SMPS works with universal input voltage range of 85 V

AC to 265 V AC. Therefore, can be used in any country and could deliver a stable output of full load within the range. For effective protection control system 2SC945 transistor is added in the design. It can operate at high voltage V_{CEO} (60 V) and have excellent linear DC current gain (2SC945 datasheet, 2014). The circuit usually samples the voltage drop across a resistor in series with switching transistor. If the current rises abnormally due to some shorted circuit, the voltage will exceed the reference level and shutdown the pulse

generator (Yusuf and Yahya, 2020). FR107 switching diode in the bulk circuit was chosen because it has high current capability and low reverse current (FR107 datasheet, 2002). Feedback is implemented to keep the output voltage fixed with line and load variations – changes due to mains voltage or load. The EL817 and Zener diode components were used for this function. EL817 photocoupler is being use as a signal transmission between circuits of different potentials and impedances (EL817 datasheet, 2013). In this study it is a link between high and low voltages.

3.3 High Frequency Transformer Design

The converter power source is the AC 110/220 V mains, and root main square (RMS), 310 V peak, at frequency of 100 kHz. The final output voltage of the charger is expected to be about 5.0 Volt and current depends on the transformer and switching transistor. The selected core is PC47EE. Operating PD is in range 85 to 220 V while the output voltage is expected to stay fixed due to feedback circuitry.

The $V_{in}(\max) = 220 \text{ V AC} = (220 \sqrt{2}) \text{ V DC} = 311 \text{ V DC}$, and $V_{in}(\text{nom}) = 85 \text{ V AC} = (85 \sqrt{2}) \text{ V DC} = 120 \text{ V DC}$ approximately. From Faraday's Law;

$$V = 4.44NAefB10^{-8} \quad 3.1$$

Where; V is the applied potential (volts RMS), 4.44 is the form factor for a sine wave while 4.0 is for square wave, N is the number of turns, A is the core cross-sectional area (cm²), f is the frequency of the oscillation (hertz), and B is the peak flux density (gauss).

The great benefit of ferrites, of course, is that they permit operation at frequencies into the hundreds of kilohertz, even to several megahertz. With the frequency very high, A and N may be set to small values, and the resulting magnetic is miniature in comparison with a low frequency device. The

number of required primary turns is calculated from equation 3.2 (Marty, B. (2005)

$$N_{pri} = \frac{V_{in}(\text{nom}) * 10^8}{4 * f * B_{max} * A_e} \quad 3.2$$

Where: N_{pri} is the number of required primary turns, $V_{in}(\text{nom})$ is nominal input voltage and A_e is effective cross-sectional area of the core in cm². The maximum flux density (B_{max}) is taken to be in the range 1300G to 2000G. This will be acceptable for most transformer cores (Majid, 2009). The oscillator's operating frequency was already chosen to be 100 kHz, while B_{max} was assumed to be 1500G. For PC47EE, the effective cross-sectional area given in the datasheet is 12.1 mm². To the nearest whole number N_{pri} was found to be 165 turns. The transformer output has to be greater than 5.0 V, due to voltage drop across the output rectifiers. Therefore, the transformer output must be $[5.0 + (\text{Total Voltage Drop Due to rectifier Diode})]$ at all input voltages. Hence, transformer output was rated at 6.5 V to compensate for this drop. To allow gab for the dead time, the Pulse Width Modulation (PWM) controller was chosen to be 98% maximum duty cycle. At a maximum duty cycle of 98%, the average voltage of the transformer is $0.98 * 120 \text{ V} = 117.6 \text{ V}$. The ratio of primary to secondary is $117.6 \text{ V} / \sqrt{2} * 6.5 \text{ V} = 12.8$, which is the turns ratio (N). Therefore; $N_{sec} = N_{pri} / N = 165 / 12.8$ is approximately 13 turns. For effective feedback axillary winding was made to tally with that of secondary. The feedback keeps the output voltage fixed with line and load variations – changes due to mains voltage or load. EL817 and Zener diode components were used for this function. In this study the Photocoupler is used as a link between high and low voltages.

The materials used in system construction were listed in table 3.1, while the circuit diagram prepared with “National Instruments NI MUTISIM”, is presented in Figure 3.2

Table 3.1: Materials used for construction

S/N	Component	Description	Quantity
1	Transistor	MJE13001	1
2	Transistor	2SC945	1
3	Photocoupler	EL817	1
4	Zener Diode	1N4733A	1
5	Diode	1N14004	1
6	Diode	FR107	1
7	LED	Green	1
8	Capacitor	4.7 μF	1

S/N	Component	Description	Quantity
9	Capacitor	220 μ F	1
10	Capacitor	10 μ F	1
11	Capacitor	1 nF	1
12	Capacitor	10 nF	1
13	Resistor	2.2 M Ω	1
14	Resistor	470 Ω	1
15	Resistor	10 Ω	1
16	Resistor	4.7 Ω	1
17	Ferric core	PC47EE	1

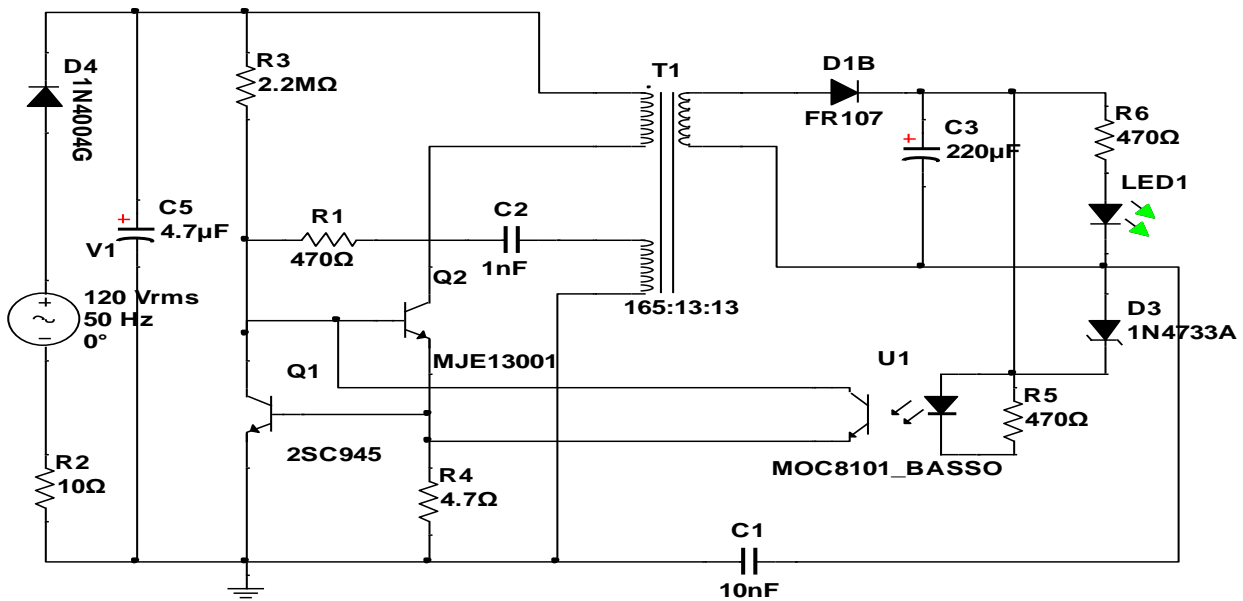


Figure: 3.2 Complete Circuit Design

3.4 System Construction

The components: transistors, diodes, capacitors, relay, and resistors were first tested individually to ascertain their working conditions. Continuity test was conducted for the diodes and transistors using a digital multimeter. The values of the resistors were also found to be within their tolerance value. Tips of the components were thinned using lead for easier soldering. One after the other, the components were soldered to their places in the

circuit. Continuity test was also conducted using the multimeter to ensure that the joints are properly done. During the soldering the active components such as the diodes and transistor, were held by the pliers to help radiate the heat quickly. Primary winding of the transformer core done first, followed by that of the secondary and lastly the feedback coil. An insulation tape was used in between the windings. The components were also fixed and soldered on plane Vero board as shown in plate (I)

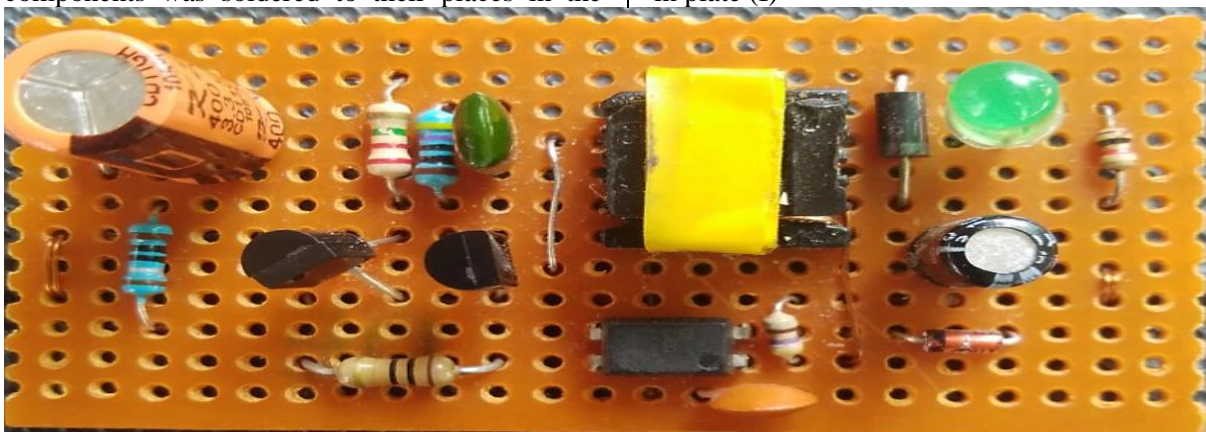


Plate: (I) Photograph of the constructed circuit

Simulation test was conducted at the transformer's primary and secondary windings and the final stage of the charger circuit as shown in figure 4.1a, b and c

4. RESULTS AND DISCUSSION

4.1 Simulations Test Results

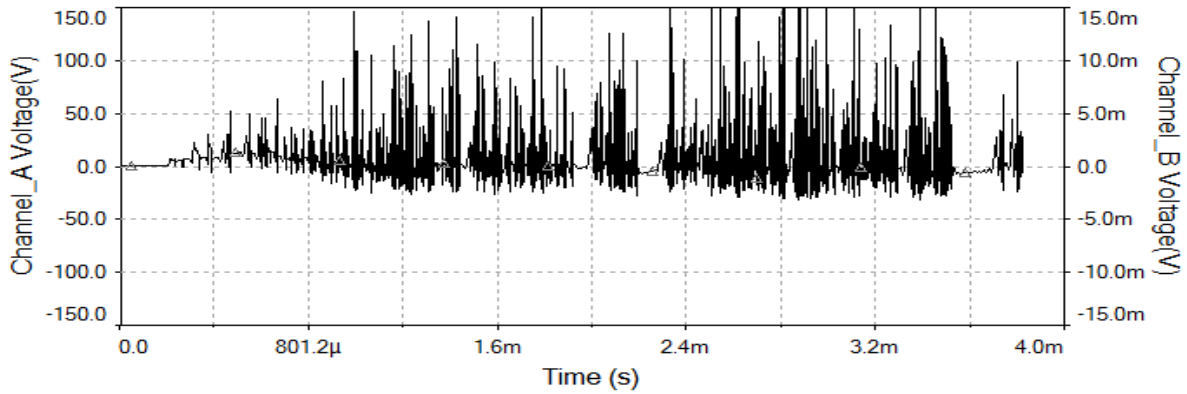


Figure: 4.1a Analogue Simulations of Primary winding in MULTISIM

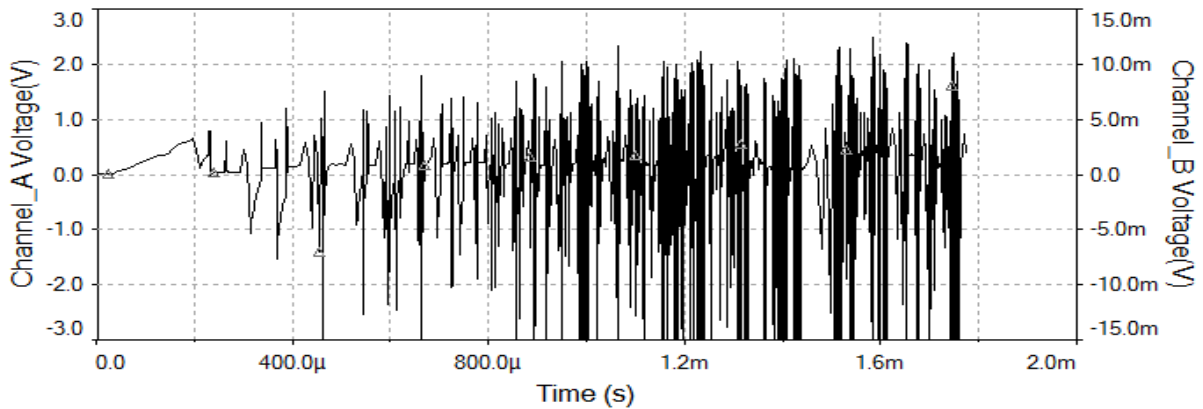


Figure: 4.1b Analogue Simulations of secondary winding in MULTISIM

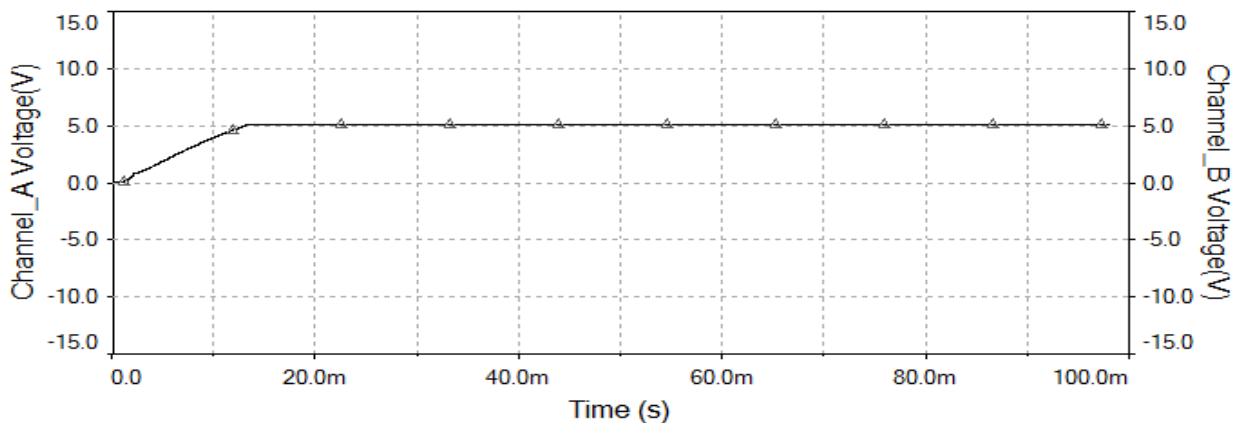


Figure: 4.1c Simulations of the charger output in MULTISIM

The results show random fluctuations in voltage in pins noise. The potential difference and frequency of the oscillator was found to be rising and falling as shown in figure 4.1a and b. The output stage was found to be 5.13 V DC for an open loop. Moreover to power sensitive electronics systems like an

amplifier, a filter circuit has to be included in the design. For battery charging the circuit is okay. The result shows that the circuit is working as projected.

4.2 System Tests

After construction, the circuit was tested to ascertain its working conditions. The charger output found to be 5.17 V DC. The output PD was also found to be steady for an input supply between 60 and 220 volt. AN attempt was made to find the output power. A wire wound variable load resistor

was connected across the output (inductive and capacitive loads were assumed to be negligible) of the charger. The Potential differences with respect to resistances were observed. The results was tabulated and represented graphically as shown in figure 4.2.

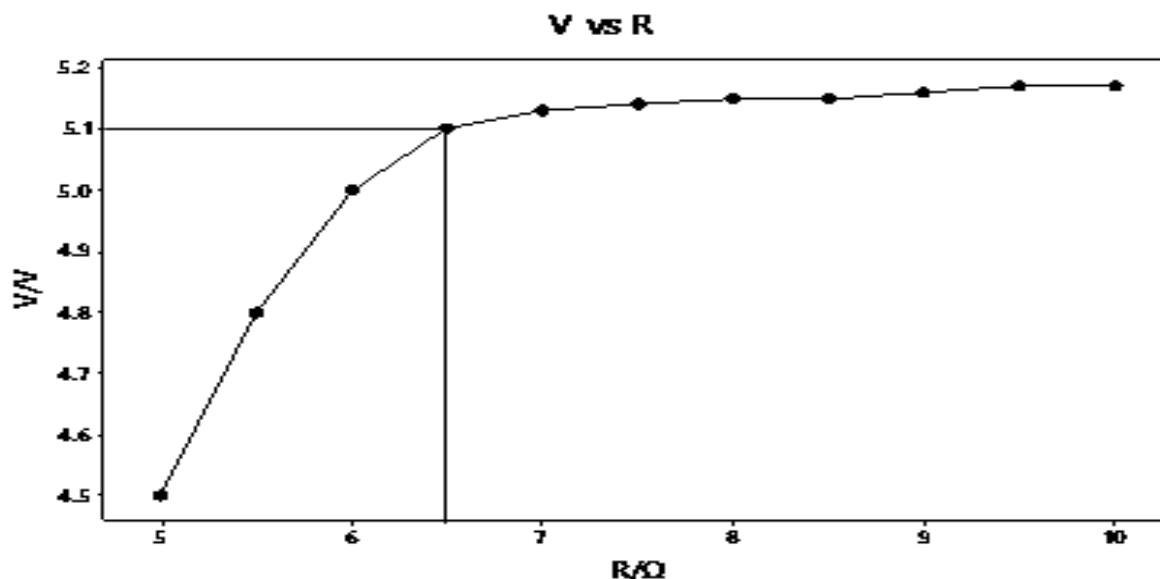


Figure 4.2: Charger PD VS Load Resistance

Figure 4.2 shows that the output PD is proportional to the load resistance. For the smooth working condition of system the output PD should not be less than 5.1 volt (Zener voltage). 5.1 volt was achieved only when the load resistance is 6.5 ohms and above. Below 6.5 ohms the PD drops below 5.1 V, which is an indication that the circuit is overloaded. In an overloaded stage, the current developed may cause transistor T_1 to conduct as a result the base of transistor T_2 will be grounded. Hence shutdown the pulse generator (T_2), and protect the whole system from being damage. For better performance the resistance load should be greater or equal to 6.5 ohms. From equation 2.1 conclusions was be made, that the power of the charger is 4 watt.

5.0 CONCLUSION

The handset charger operates on input voltages ranging from 85 to 220 volt with a charging PD of 5.1 V DC. It was tested on different cell phones (Itel S15, Tecno L8, K7, Gionee S11 Lite, S10 Lite Samsung Galaxy M40, and Infinix S4) and found to be working properly. Applying equation 2.1 to what obtained in Figure 4.2, the maximum output power was found to be 4 watt. From the analysis and tests conducted, the charger was found to be working as anticipated.

REFERENCES

- 2SC945 Datasheet, (2014). Audio Frequency Amplifier High Frequency OSC NPN Transistor, Unisonic Technologies co., retrieved from www.unisonic.com.tw.
- Brown, M. (1990). Practical switching power supply design. Academic Press A Harcourt Science and Technology Company San Diego, California ISBN 0-12-137030-5. USA, Retrieved from <http://www.apnet.com>
- Christine, Y. (2011). Simple Circuit Charges Lead-Acid Batteries, Application Note 621, Maxim Integrated, Retrieved from: <http://www.maximintegrated.com/an621>
- Crosby, G. & Deppong, J. (2013). Design And Testing of a Wireless Phone Charger, Technology Interface International Journal 14, No. 1 (Jan 2013): 45-52.
- EL817 Datasheet, (2013). 4 pin DIP phototransistor photocoupler. Ever Light Corporation, Retrieved from www.everlight.com.
- FR107 Datasheet, (2002). Fast Recovery Rectifier Diode EIC Dig Chip, Retrieved from <http://www.digchip.com>.
- Francisco, O., Ronald Q., Constantino, M., and Soriano, P. (2019). International Journal of Innovative Technology and Exploring

- Engineering (IJITEE) ISSN: 2278-3075, Volume-9 Issue-2, December 2019.
- Humphreys J., Hammerton C.J., Brown D., Miller R., Burley L., (1994) "Power Semiconductor Applications-Switched Mode Power Supplies", Philips Semiconductors, Chapter 2, Hamburg.
- Joe L. P., Sasirekha S., Naveen D K D., Revanth P S. (2018). Working model for mobile charging, using wireless power transmission. *International Journal of Engineering and Technology* 7(3.12):548 DOI:10.14419/ijet.v7i3.12.16434
- Kharudin, A., Wan Syahidah, W M., Ammar, A. (2016). Design and implementation of portable mobile phone charger using multi directional wind turbine extract. *Indian Journal of Science and Technology*, DOI: 10.17485/IJST/2016/V9I9/88711, Corpus ID: 54016321)
- Lou, F. (2017). Power Topology. *Electronic Design note* 162070717i. Retrieved from <http://www.electronicdesign.com/power/16-ways-design-switch-mode-power-supply>
- Majid, D. (2009). From Powder to Transformer, Fairchild Semiconductor Power Seminar (2008 – 2009) pp 2.
- Marty, B. (2005). Publication Order Number AND8039. ON, Semiconductor Components Industries, LLC, [Online] Retrieved Jan, 3 201 Retrieved from <http://onsemi.com>.
- MJE13001 Datasheet, (2015). NPN Silicon Power, Transistor Unisonic Technologies Co., Retrieved from www.unisonic.com.tw.
- Shobana, G. & Suguna, M. (2019). Smart Equipment Charger, *International Journal of Engineering and Advanced Technology (IJEAT)* ISSN: 2249 – 8958, Volume-8 Issue-6S.
- Venkatesh K. L., and Chappidi S., (2015). Design of a Portable USB Mobile Charger, *international journal of recent contributions from engineering and IT (iJES)* <http://dx.doi.org/10.3991/ijes.v3i3.4937>
- Yusuf, Y. & Yahya, H N. (2020). Design, Construction and Evaluation of 5A AC-DC Portable Lead Acid Battery Charger with an Inbuilt Automatic Shut OFF. *International Journal of Science for Global Sustainability* Vol. 6(2) July, 2020 Pg 126-134